Neurobiology of Aging 73 (2019) 200–210

Contents lists available at ScienceDirect

Neurobiology of Aging

journal homepage: www.elsevier.com/locate/neuaging

Effects of estrogen and aging on synaptic morphology and distribution of phosphorylated Tyr1472 NR2B in the female rat hippocampus

Elizabeth M. Waters [a], Sanoara Mazid [a], Mariana Dodos [b], Rishi Puri [c], William G. Janssen [c], John H. Morrison [d], Bruce S. McEwen [a,1], Teresa A. Milner [a,b,*,1]

[a] Laboratory of Neuroendocrinology, The Rockefeller University, New York, NY, USA
[b] Feil Family Brain and Mind Research Institute, Weill Cornell Medicine, New York, NY, USA
[c] Fishberg Department of Neuroscience and Friedman Brain Institute, Icahn School of Medicine at Mount Sinai, New York, NY, USA
[d] Department of Neurology, Center for Neuroscience, The California National Primate Research Center, UC Davis, Davis, CA, USA

ARTICLE INFO

Article history:
Received 28 April 2017
Received in revised form 10 August 2018
Accepted 18 September 2018
Available online 25 September 2018

Keywords:
Estrogen deprivation
Hormone replacement
Presynaptic glutamate receptors
CA1 region
Aging

ABSTRACT

Age and estrogens may impact the mobility of N-methyl-D-aspartate receptors (NMDARs) in hippocampal synapses. Here, we used serial section immunogold electron microscopy to examine whether phosphorylated tyrosine 1472 NR2B (pY1472), which is involved in the surface expression of NMDARs, is altered in the dorsal hippocampus of young (3–4 months old) and aged (~24 months old) ovariectomized rats treated with 17β-estradiol or vehicle for 2 days. The number of gold particles labeling pY1472 was higher in presynaptic and postsynaptic compartments of aged rats with low estradiol (vehicle-treated) compared to other groups. In terminals, pY1472 levels were elevated in aged rats but reduced by estradiol treatment to levels seen in young rats. Conversely, the mitochondria number was lower in aged females but was restored to young levels by estradiol. In the postsynaptic density and dendritic spines, estradiol reduced pY1472 in young and aged rats. As phosphorylation at Y1472 blocks NR2B endocytosis, reduction of pY1472 by estradiol suggests another mechanism through which estrogen enhances synaptic plasticity by altering localization of NMDAR subunits within synapses.

1. Introduction

The ability of estrogen levels to regulate hippocampal function and structural characteristics has been studied for more than three decades in female rodents. In both rodents and nonhuman primates, hippocampal synapse density increases on CA1 pyramidal cell basal dendrites when estrogen levels are highest (Hao et al., 2003; Woolley and McEwen, 1992). However, this estrogen effect is limited in rodents to young adult females as estrogen fails to increase CA1 synapse density in aged female rats (Adams et al., 2001c), although spinophilin labeling, a key marker of spines, is maintained throughout adult life in nonhuman primates (Hao et al., 2003). Changes in estrogen's ability to maintain synapses and promote synapse formation may be due to changes in estrogen receptor (ER) expression as synaptic ERα decreases but ERβ persists in CA1 synaptic profiles of aged rats (Adams et al., 2002; Foster, 2012; Waters et al., 2011). Because ERs have been shown to regulate synaptic protein levels in CA1, CA3, and the hilus of the dentate gyrus (Brake et al., 2001; Waters et al., 2009) and second messenger pathways are implicated in synapse formation and maintenance (Akama and McEwen, 2003; Bean et al., 2014; Foster, 2012; Hasegawa et al., 2015; Kramar et al., 2013; Tuscher et al., 2016; Znamensky et al., 2003), the loss of ERs, and the concomitant reduction in estrogen sensitivity of the brain has far ranging implications for synaptic health during aging.

Estrogen-mediated synapse formation coincides with improved learning and memory in adult females and disruption of this effect through inhibition via estrogen activation of signaling pathways or interactions with N-methyl-D-aspartate receptors (NMDARs) prevents synaptic plasticity and enhanced cognitive performance (Bean et al., 2014; Lewis et al., 2008; Smith and McMahon, 2006; Vedder et al., 2013; Woolley and McEwen, 1994). In adults, NMDARs comprise two obligatory NR1 subunits and two regulatory subunits, mainly NR2A and NR2B (Cull-Candy and Leszkiewicz, 2004; MacDonald et al., 2006). NMDAR subunit expression and localization within synapses is altered by estrogen in young and

* Corresponding author at: Feil Family Brain and Mind Research Institute, Weill Cornell Medicine, 407 East 61st St, Room 307, New York, NY 10065, USA. Tel.: 646-962-8274; fax: 646-962-0535.
E-mail address: tmilner@med.cornell.edu (T.A. Milner).
[1] Co-principal investigators.

0197-4580/$ – see front matter © 2018 Elsevier Inc. All rights reserved.
https://doi.org/10.1016/j.neurobiolaging.2018.09.025

aged female rats (Adams et al., 2001a, 2004). Expression levels of NMDAR subunits along with post-translational modifications ultimately regulate the ability of NMDAR to detect glutamate and affect synaptic responsiveness (Hunt and Castillo, 2012). NMDAR subunits contain many serine/threonine and tyrosine phosphorylation sites that are substrates for several kinases including cAMP-dependent protein kinase A and CAMKII; interactions between NMDAR and these kinases underlie many forms of synaptic plasticity (Chen and Roche, 2007).

Within the postsynaptic density, the NR2B subunit of the NMDAR is the predominant tyrosine-phosphorylated protein (Moon et al., 1994). Try1472 (Y1472) is the major phosphorylation site within NR2B (Nakazawa et al., 2001; Takasu et al., 2002). Phosphorylation of NR2B at Y1472 is low at the baseline but acutely and rapidly increases after long-term potentiation (LTP); this is important for surface expression of NMDARs and contributes to NMDAR activation (Lu et al., 2015; Nakazawa et al., 2001; Nong et al., 2004; Prybylowski et al., 2005), whereas inhibition of tyrosine phosphorylation reduces LTP facilitation (Chen et al., 2014). In the hippocampus, altered tyrosine phosphorylation of NMDARs would presumably be involved in the cognitive decline associated with normal aging and neurodegenerative diseases such as Alzheimer's disease (Foster et al., 2017; Guidi et al., 2015).

The current experiment hypothesized that 17β-estradiol (E2) treatment and age would interact in the regulation of synaptic morphology and composition, including mitochondria and phosphorylated Y1742 NR2B (pNR2B) levels and distribution. Together with our previous findings that age altered ER expression and regulation within synapses (Adams et al., 2002; Waters et al., 2011) and estrogen's ability to modulate NR2B mobility within the synapse regardless of age (Adams et al., 2004), the current question had important implications for estrogen replacement in the context of age when estrogen levels and hippocampal dependent functions decline. The hippocampus of young and aged female rats that were ovariectomized and treated with vehicle (Veh) or E2 was analyzed by quantitative three-dimensional electron microscopy to identify the characteristics of synapses in the CA1 stratum radiatum and the distribution of phosphorylated Try1472 NR2B immunoreactivity within the synapses.

2. Materials and methods

2.1. Animals

All experiments were approved by the Icahn School of Medicine at Mount Sinai Institutional Animal Care and Use Committee and were conducted in accordance with the National Institutes of Health Guide for the Care and Use of Laboratory Animals. Young (3–4 months; 225 grams; N = 11) and aged (23–24 months; 350 grams; N = 11) adult female Sprague Dawley rats from Harlan (Indianapolis, IN) were used in these studies. The young females were virgins, and the aged females were either virgins or retired breeders (Adams et al., 2002). Animals were housed in a temperature-controlled room (12-h light/dark cycle; lights on at 0700). Food and water were available *ad libitum*. The tissue samples used in the electron microscopic experiments were from the same rats as those used in previous studies (Adams et al., 2001c, 2002, 2004; Waters et al., 2011; Yildirim et al., 2008).

2.2. Experimental groups

Before bilateral ovariectomy (OVX), young rats exhibited regular estrous cycles and aged rats were acyclic (i.e., constant estrous or diestrus) (Adams et al., 2001a), thus the time from the last estrogen exposure to the onset of estradiol treatment after OVX varied for the young and aged females. Estradiol replacement began seven days after OVX, when a silastic capsule (outer diameter 3.18 mm; inner diameter 1.96 mm) filled with either E2 (10% in cholesterol) or cholesterol (Veh) was implanted subcutaneously. To account for differences in body weight, implants in young rats were 1 cm in length and implants in aged rats were 2 cm in length (Funabashi et al., 1998; Lauber et al., 1990). In previous studies using this E2 replacement paradigm in long-term ovariectomized aged rats, a similar uterine response was observed and the circulating estradiol levels were within the physiological range (Adams et al., 2001b).

2.3. Tissue preparation and embedding

Two days after the capsules were implanted, rats were anesthetized with 30% chloral hydrate (i.p.) and perfused transcardially with 2% dextran in 0.1 M phosphate buffer (PB) (pH 7.4, 50 mL/min) for 1 minute, followed by 4% paraformaldehyde and 0.125% glutaraldehyde in PB for 10–15 minutes (Adams et al., 2001c). The brains were removed and postfixed overnight in the last fixative. One block from the dorsal hippocampus (1 mm thick) was randomly selected from 4 rats per group to be processed for embedding. Freeze substitution and low-temperature embedding of the specimens were performed as described previously (Adams et al., 2002; Janssen et al., 2005; Van Lookeren Campagne et al., 1991). Initial cryoprotection consisted of immersing sample hippocampal blocks in increasing concentrations (10, 20, and 30%) of glycerol in PB and then rapidly plunging in liquid propane cooled by liquid nitrogen (-190°C) in a Universal Cryofixation System KF80 (Reichert-Jung, Vienna). For *en bloc* fixation, samples were immersed in 1.5% uranyl acetate in anhydrous methanol (-90°C, 24 hours) in a cryosubstitution Automatic Freeze Substitution System unit (Leica, Vienna) while the temperature was increased in steps of 4°C/h from -90 to -45°C. After a wash with anhydrous methanol, samples were infiltrated with Lowicryl HM20 resin (electron microscopy sciences [EMS]) at -45°C with a progressive increase in the ratio of resin to methanol for 1 hour each, followed by pure Lowicryl overnight. Polymerization was performed with UV light (360 nm) at -45°C for 48 hours, followed by 24 hours at room temperature.

A rectangular area of the dorsal hippocampal CA1 (~400–500 μm long x 200–250 μm wide) that contained the pyramidal cell layer and stratum radiatum was trimmed with a Mesa knife (EMS) on a UTC Leica Ultramicrotome. Five-six consecutive ultrathin sections were then cut at 80-nm thickness using a DiATOME diamond knife (EMS) and mounted on formvar/carbon-coated 2x1 mm oval slot nickel grids (EMS).

2.4. Phosphorylated Tyr1472 NR2B antibody

A polyclonal rabbit antibody to the phosphopeptide corresponding to the amino acid residues surrounding the phospho-Tyr1472 of NMDA NR2B was used in these studies (pNR2B; PhosphoSolutions p1516-1472). In Western blots of rat hippocampal lysates, this antibody immunolabels the ~180k NR2B subunit of the NMDAR phosphorylated at Tyr1472 (Gladding et al., 2012; Hicklin et al., 2011). Immunolabeling for the antibody is blocked by treatment of hippocampal lysates with lambda phosphatase and by preadsorption with the phosphopeptide used as the antigen but not the corresponding dephosphopeptide (manufacturer's data sheet).

2.5. Postembedding immunogold electron microscopic labeling

For immunolabeling, the grids with ultrathin sections were treated with a saturated solution of NaOH in absolute ethanol, rinsed, and incubated at room temperature in 0.1% sodium

borohydride and 50 mM glycine, followed by Tris-buffered saline (TBS) containing 2% human serum albumin (HSA). The grids then were incubated overnight with the pNR2B antibody (1:50 dilution) in the TBS/HSA solution. The next day, the grids were washed and incubated in secondary 10 nm gold-tagged goat-anti-rabbit IgG F(ab')$_2$ antibody (EMS) diluted 1:75 in TBS with 2% HSA and 5 mg/mL polyethylene glycol 20,000 Da. The dilutions of the primary and secondary antibodies first were determined empirically. Sections were washed and dried, then counterstained with 1% uranyl acetate and Reynolds lead citrate.

2.6. Electron microscopic analysis

2.6.1. Data collection

A person blind to the group identity performed all data collection and analyses. The primary goal of the present study was to provide a detailed characterization of the patterns of pNR2B immunolabeling within synaptic complexes for each experimental group. For this, protein distribution for pNR2B in synaptic profiles of different sizes, rather than the number of gold particles or synaptic profiles per animal, is analyzed. Similar to previous studies from our group (Crimins et al., 2017; Hara et al., 2014), the sections were collected using a systematic-random approach on an HF2000 transmission electron microscope (Hitachi High Technologies America, Inc.). To ensure that images were taken from stratum radiatum, photographs were captured in the middle of a region 100–200 μm below the bottom of the pyramidal cell layer. Images were captured at a direct magnification of 17,000 with a digital camera system (v3.2 Advanced Microscopy Techniques, Danvers, MA) using Photoshop to assist with aligning the serial sections.

Four blocks from each experimental group (N = 4/group) were photographed and analyzed: (1) young OVX + Veh; (2) young OVX + E; (3) aged OVX + Veh; and (4) aged OVX + E. For each block, 5 serial images from 10 random fields (total 50 μm^2/field) were collected in stratum radiatum located 50–150 μm below the pyramidal cell layer. The middle section was considered section 0 and then sections above this section were labeled +1 and +2, whereas the sections below this section were labeled -1 and -2. Before analysis, synaptic complexes that consisted of a terminal, synaptic specialization and dendritic spine were identified and numbered in section 0. Synapses that lacked clear visualization and delineation of classic synaptic structures such as presynaptic and postsynaptic membranes, a synaptic cleft, and postsynaptic density (PSD) were excluded from the quantitative analysis. Using this approach, approximately 100 synaptic complexes were collected for each block.

2.6.2. PSD measurement

The size and area of PSD formed between pNR2B-containing terminals and/or pNR2B-containing dendritic spines were measured using the ruler tool in Adobe Photoshop CS5 (version 12.0 x64, Adobe systems incorporated). For this, the PSD length was taken on the one section with the longest length, and the area was determined by combining the PSD length from all sections with the spine multiplied by the section thickness.

2.6.3. Mitochondrial distribution and volume

The number and volume of the mitochondria in profiles labeled for pNR2B were measured using the ruler tool in Adobe Photoshop. The volume was calculated using the measured diameter of the mitochondria in each section it appeared and the section thickness.

2.6.4. Analysis of synaptic distribution of pNR2B gold particles

Six zones were defined for each synaptic complex: (1) the presynaptic terminal zone across from the PSD extending 0–60 nm from the inner border of the presynaptic membrane; (2) the presynaptic terminal zone >60 nm from the inner border of the presynaptic membrane; (3) the synaptic cleft; (4) on the PSD; (5) near PSD from 30–60 nm of the postsynaptic membrane; (6) the dendritic spine cytoplasm which included regions >60 nm from the PSD. A dendritic spine or presynaptic terminal was considered labeled if one or more gold particles were present anywhere within it or in the synaptic cleft. Immunogold particles were summed in all planes of a section that contained a given synaptic complex (Fig. 1).

2.7. Statistical analysis

Statistical analyses were performed using JMP 12 (SAS Institute Inc., Cary NC). The coefficients of variation (CV = standard deviation/mean) and coefficient error were calculated. Potential group differences in percentage of labeled synapses and the number of gold particles per synaptic compartment between young OVX Veh- and estrogen-treated rats, as well as aged OVX Veh- and estrogen-treated rats, were evaluated by two-way analysis of variance

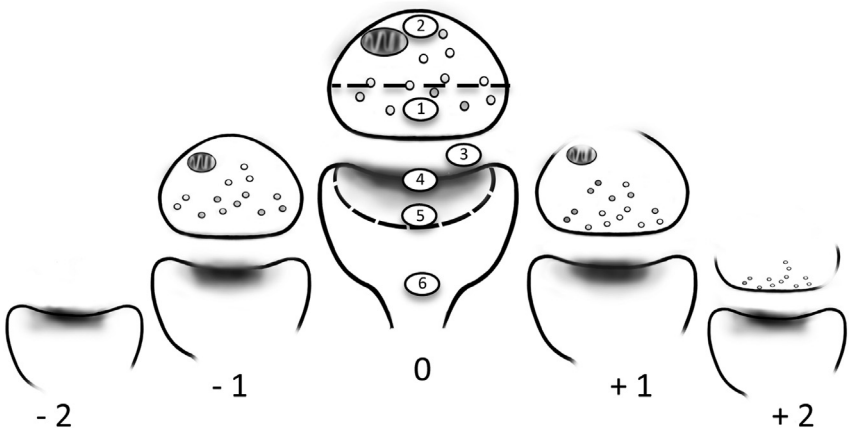

Fig. 1. Schematic illustrating the serial section analysis used to determine pNR2B gold particle location within synaptic complexes. Synaptic complexes were analyzed in five serial sections: middle section = section 0; sections above middle section = +1 and +2; sections below middle section = −1 and −2. Six zones (center) were analyzed: (1) the presynaptic terminal zone across from the postsynaptic density (PSD) extending 0–60 nm from the inner border of the presynaptic membrane; (2) the presynaptic terminal zone >60 nm from the inner border of the presynaptic membrane; (3) the synaptic cleft; (4) on the PSD in the postsynaptic dendritic spine; (5) near PSD from 30–60 nm of the postsynaptic membrane; and (6) the cytoplasm of the dendritic spine which included regions >60 nm from the PSD.

(ANOVA). The grouped data also were compared by two-way ANOVA, and multiple comparisons were made by Tukey-Kramer adjustments. Significance was set at $p < 0.05$. All values are given as means ± SEM.

All images were captured and further processed by using the Adobe Photoshop CS5 program. Only minor adjustments of brightness, contrast, and sharpening were made, which in no case altered the appearance of the original material.

3. Results

3.1. E2 regulated spine morphology in young but not aged females

In the hippocampus, several types of dendritic spines, including thin, stubby, mushroom, and branched (Bourne and Harris, 2008; Lee et al., 2012), are found opposed by axon terminals of similar size. For each CA1 stratum radiatum pNR2B-labeled synapse, the spine and presynaptic terminal diameters were analyzed from the section (-2, -1.0, +1, +2) with the largest diameter compared to all sections where the same synaptic complex was identifiable.

For the diameter of pNR2B-containing axon terminals, there were main effects of E2 treatment [$F(1,1521) = 9.77$, $p = 0.0018$] as well as age x E2 treatment [$F(1,1521) = 4.44$, $p = 0.0353$]. Post hoc tests showed that E2 treatment significantly increased pNR2B-containing terminal diameter in young females ($p = 0.0015$) and in aged females ($p = 0.0154$) compared to the Veh-treated young females (Fig. 2A).

The diameter of pNR2B-containing dendritic spines differed between treatment groups; there were significant main effects of age [$F(1,1455) = 12.20$, $p = 0.0005$] and E2 treatment [$F(1,1455) = 5.03$, $p = 0.0251$; Fig. 2B]. Post hoc analyses indicated that, compared to young + Veh, mean spine diameter increased in aged + Veh ($p = 0.0496$) and aged + E2 ($p = 0.0003$) groups (Fig. 2B).

Neither the PSD length (Fig. 2C) nor the PSD area (Fig. 2D) formed between pNR2B-containing terminals and/or pNR2B-containing dendritic spines was significantly different between any of the experimental groups.

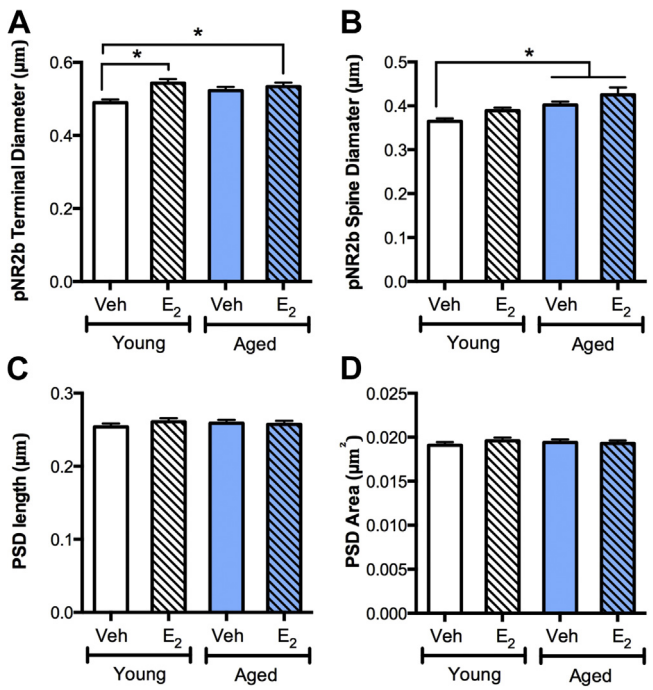

Fig. 2. Morphological changes in pNR2B-labeled synaptic complexes related to age and E2 treatment. (A) The diameter of pNR2B-containing terminals was increased in young + E2 females and in both aged female groups compared with young + Veh. There was no difference in pNR2B-containing diameter between aged females with E2 or Veh. (B) Compared to young + Veh females, the diameter of pNR2B-containing dendritic spines increased in aged females regardless of treatment. (C and D) The length and area of PSDs formed between pNR2B-containing presynaptic and/or postsynaptic profiles were not altered by age or treatment. N = 4 rats/group; n ~ 100 synaptic profiles/rat; *$p < 0.05$. Abbreviations: E2, 17β-estradiol; Veh, vehicle; PSD, postsynaptic density.

3.2. E2 restored mitochondria in aged female axon terminals

In all four experimental groups, mitochondria were found presynaptically (Fig. 3A) and postsynaptically (Fig. 3B) in pNR2B-

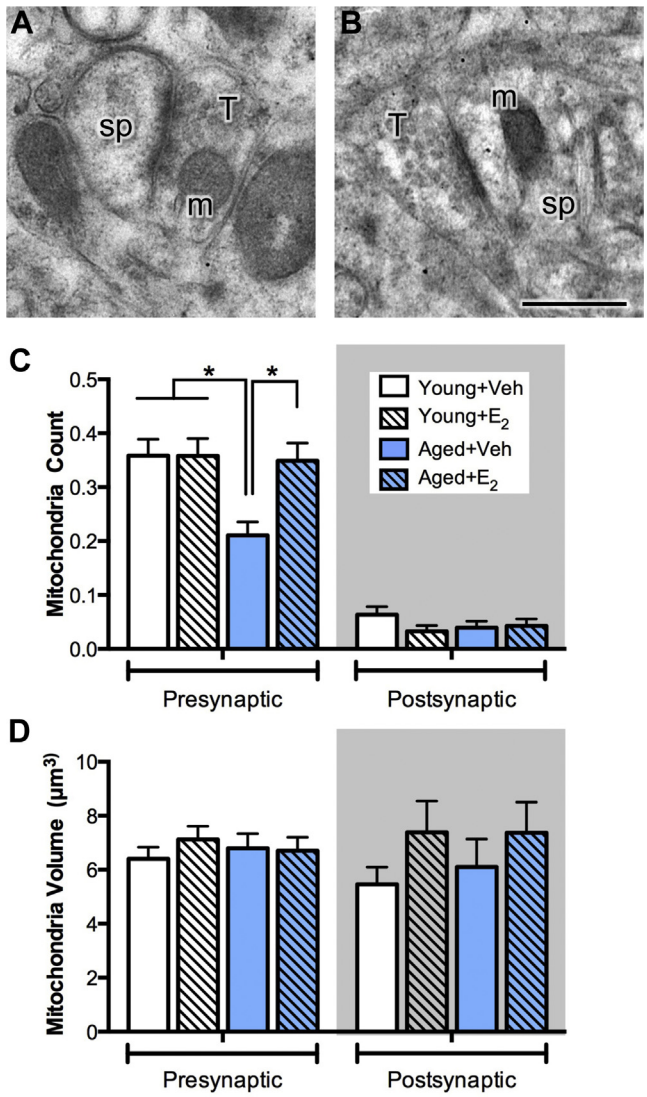

Fig. 3. Mitochondrial counts, but not morphology, in pNR2B-labeled presynaptic profiles differed with aged and estradiol treatment. (A and B) Representative electron micrographs show mitochondria in presynaptic (A) and postsynaptic (B) profiles. Scale bar, 500 nm. (C) The number of mitochondria in presynaptic NR2B-labeled profiles is significantly decreased in aged + Veh females compared to both groups of young females but significantly increased after E2. There was no significant difference in the number of mitochondria in postsynaptic profiles in all 4 groups. (D) Mitochondrial volume was not altered by age or treatment in presynaptic or postsynaptic compartments of pNR2B-labeled profiles. N = 4 rats/group; n ~100 synaptic profiles/rat; *$p < 0.05$. Abbreviations: m, mitochondria; sp, dendritic spine; T, axon terminal; E2, 17β-estradiol; Veh, vehicle; PSD, postsynaptic density.

containing synaptic complexes. Examination of the mitochondria number in presynaptic pNR2B-containing profiles showed significant main effects of age [F(1,1203) = 6.80, $p = 0.0092$] and E2 treatment [F(1,1203) = 5.19, $p = 0.0229$]. Moreover, the interaction of age and treatment factors with regard to the mitochondria number also was significant [F(1,1203) = 5.25, $p = 0.0221$]. In postsynaptic pNR2B-containing profiles, there were no significant main effects or interactions in the number of mitochondria.

In the pNR2B-labeled terminals, post hoc analysis showed that aged + Veh females had significantly fewer mitochondria than aged + E2 ($p = 0.0081$) and both young + Veh and young + E2 treated groups ($p = 0.0026$, $p = 0.0029$, respectively; Fig 3C left). In contrast, the number of mitochondria was not significantly different in young + Veh females compared to young + E2 females. Although the number of mitochondria decreased in aged + Veh females compared to the other three groups, total mitochondrial volume did not change overall in pNR2B containing presynaptic profiles (Fig 3D). Moreover, postsynaptic mitochondria pNR2B profiles were not changed after E2 in young or aged females (Fig. 3C right).

Mitochondria change their shapes through the combined actions of fission, fusion, and motility (Youle and van der Bliek, 2012). Fission generates new organelles, which are usually small and round; fusion allows functional mitochondria to combine with dysfunctional mitochondria and share components, generally resulting in larger mitochondria (Youle and van der Bliek, 2012). To address the possibility that mitochondrial fission or fusion was affected by age and/or treatment, the ratio of the form factor to total mitochondria volume in pNR2B-containing profiles was examined in each group. No changes in mitochondrial forms were detected in presynaptic or postsynaptic profiles of any group (data not shown).

3.3. Overall, age increased and E2 decreased pNR2B gold particle labeling

In the CA1 stratum radiatum, pNR2B gold labeling was found in synaptic complexes consisting of presynaptic axon terminals (Fig. 4A, top) and postsynaptic dendritic spines (Fig. 4A, center). These labeled terminals and spines opposed unlabeled profiles as well as pNR2B-labeled profiles (Fig. 4A, bottom). Total pNR2B gold particle number in terminals and spines showed significant main effects of age [F(1,1632) = 7.12, $p = 0.0077$] and E2 treatment [(F1,1632) = 11.36, $p = 0.0008$], but there were no significant interactions between age and E2. Post hoc analysis showed that aged + Veh females had increased pNR2B gold particles compared to young + E2 females ($p = 0.0001$); however, there was no significant increase compared to aged + E2 females ($p = 0.0678$; Fig. 4B).

In the synaptic complexes in which pNR2B gold particles were only in terminals, there was a significant main effect of E2 treatment [F(1,303) = 5.62, $p = 0.0184$] due to decreased labeling in young and aged E2-treated rats. The post hoc analysis showed that young + E2 and aged + E2 had significantly less pNR2B gold particles in synaptic complexes than aged + Veh ($p = 0.0265$ and $p = 0.0339$, respectively; Fig. 4C left). Synaptic complexes containing pNR2B labeling only in the postsynaptic spine profiles had no main effects or interactions of age or E2 treatment (Fig 4C center). In synaptic complexes in which both presynaptic and postsynaptic profiles were labeled, there were significant main effects of age [F(1,480) = 6.99, $p = 0.0084$] and E2 treatment [F(1,480) = 5.26, $p = 0.0222$] but no interaction between age and treatment. Post hoc analyses showed that aged + Veh females had significantly more synaptic complexes with pNR2B gold particles in both presynaptic and postsynaptic profiles compared to the young + Veh females ($p = 0.0382$) and young + E2 females ($p = 0.0042$; Fig. 4C right).

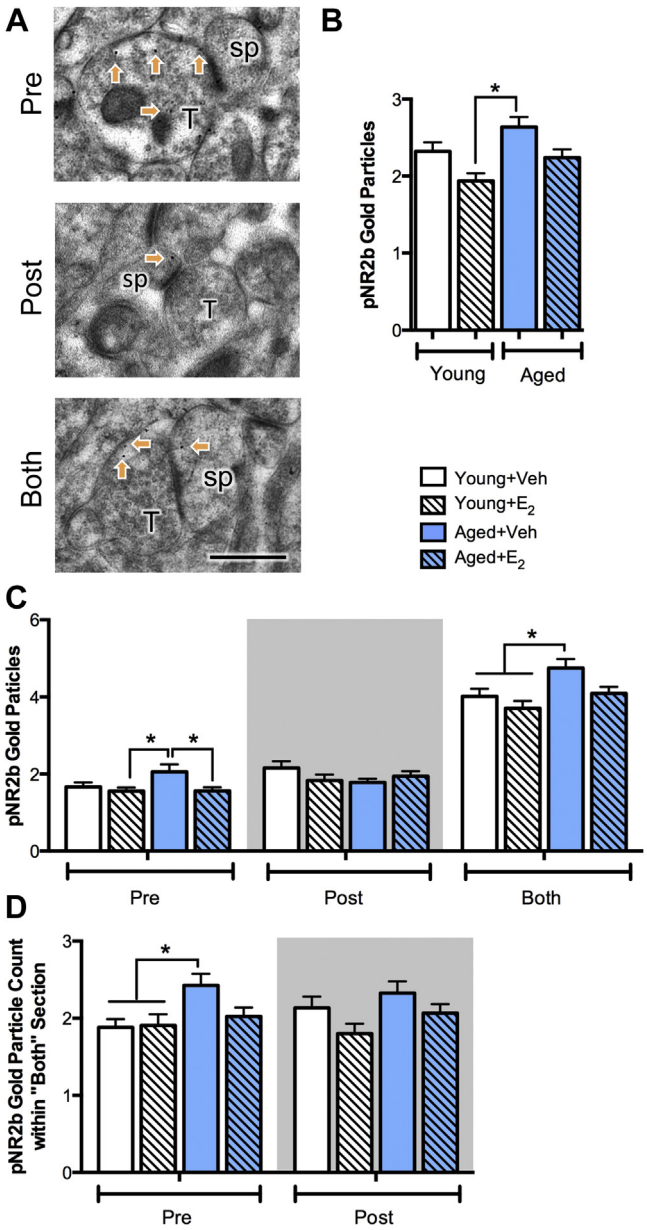

Fig. 4. Age and E2 treatment affected the number of pNR2B gold particles in presynaptic and postsynaptic profiles. (A) Electron micrographs show examples of synaptic complexes with pNR2B gold particles in only presynaptic profiles (top), only postsynaptic profiles (middle), or both presynaptic and postsynaptic profiles (bottom). Scale bar = 500 nm. (B) Aged + Veh females had significantly more total pNR2B gold particles in synaptic complexes than young + E2 females. (C) In synaptic complexes with only presynaptic pNR2B-labeled profiles, aged + Veh females had significantly more pNR2B gold particles compared to young + E2 females and aged + E2 females. In synaptic complexes with only postsynaptic pNR2B-labeled profiles, there were no significant differences in the number of gold particles between any of the groups. In synaptic complexes with pNR2B labeling in both presynaptic and postsynaptic profiles, aged + Veh females had significantly more gold particles than both young female groups. (D) When synaptic complexes with pNR2B labeling in both presynaptic and postsynaptic profiles were further subdivided, aged + Veh females had significantly more pNR2B gold particles in terminal profiles compared to young + Veh and young + E2 females. N = 4 rats/group; n ~ 100 synaptic profiles/rat; *$p < 0.05$. Abbreviations: E2, 17β-estradiol; Veh, vehicle; sp, dendritic spine; T, axon terminal. (For interpretation of the references to color in this figure legend, the reader is referred to the Web version of this article.)

Within synaptic complexes where both the terminal and spine were labeled, there was a main effect of age in the presynaptic compartment [F(1,480) = 6.00, $p = 0.0146$]. Post hoc analysis

showed that the number of pNR2B gold particles in the presynaptic compartment increased in the aged + Veh group compared to both young + Veh and young + E2 ($p = 0.0112, 0.0432$), but there was no difference compared to aged + E2 ($p = 0.1090$). In addition, there were no differences between aged + E2 and both groups. The postsynaptic compartment showed a main effect of E2 treatment associated with pNR2B labeling [$F(1,480) = 4.19$, $p = 0.0412$]. Post hoc analysis showed no differences in pNR2B gold particles between any groups (Fig. 4D). However, the number of pNR2B gold particles in the postsynaptic compartment of the aged + Veh group tended ($p = 0.0643$) to be less than the young + E2 group.

3.4. E2 treatment decreased pNR2B gold particles in a compartment-specific manner

Synaptic and extrasynaptic pNR2B labeling was compared by assigning gold particles to bins determined by their distance from the PSD or synaptic cleft (Fig. 1; see detailed description in methods). Presynaptically, there was a significant main effect of age on the number of pNR2B gold particles both in the near terminal bin [$F(1,1632) = 4.17$, $p = 0.0413$] and in the synaptic cleft [$F(1,1632) = 11.84$, $p = 0.0006$]. Moreover, there was a trend [$F(1,1632) = 3.57$, $p = 0.0589$] for a main effect of age on the number of pNR2B gold particles in the far terminal bin. Post hoc analyses indicated that aged + Veh had significantly more pNR2B gold particles in the near terminal bin compared to young + Veh ($p = 0.0273$), young + E2 ($p = 0.0333$), and aged + E2 ($p = 0.0479$). In the synaptic cleft, post hoc analysis showed that aged + E2 had significantly more pNR2B gold particles compared to young + E2 ($p = 0.0028$; Fig. 5A, right) and young + Veh ($p = 0.0453$). Post hoc analyses showed a trend ($p = 0.0512$) for increased pNR2B gold particles in aged + Veh compared to the young + E2 group. In young females, E2 had no significant effect on pNR2B gold particles in the presynaptic terminal or synaptic cleft (Fig. 5A).

Postsynaptically, the number of pNR2B gold particles in bins showed significant main effects of E2 treatment in the PSD [$F(1,1632) = 17.54$, $p < 0.0001$] and spine [$F(1,1632) = 6.56$, $p = 0.0105$]. A main effect of age was present in the near PSD bin [$F(1,1632) = 10.12$, $p = 0.0015$]. No other main effects or interactions were detected. Post hoc analysis indicated that the numbers of pNR2B gold particles on the PSD compartment were elevated in young + Veh females compared to young + E2 ($p = 0.0011$) and aged + E2 treated females ($p = 0.0266$). There was a significant difference in pNR2B gold particles on the PSD compartment of aged + Veh compared to young + E2 ($p = 0.0098$) but not to aged + E2 ($p = 0.1321$). In the near PSD, aged + E2 females had significantly more pNR2B gold particles ($p = 0.0385$) than young + Veh females. In the cytoplasm of dendritic spines, the number of pNR2B gold particles tended ($p = 0.0689$) to be less in aged + E2 females compared to young + Veh females (Fig. 5C). In these compartments, there were no significant differences between aged + E2 females.

3.5. Three-dimensional reconstruction of synaptic complexes depicts changes in terminal size and pNR2B gold particle distribution related to E2 status and age

The relation of pNR2B gold particles within one representative synaptic complex from each group is shown by three-dimensional reconstruction (Fig 6). In all four groups, mitochondria are found primarily in presynaptic terminals. The terminal diameter of the young + Veh group was less than that in the young and aged + E2 group, whereas the PSD length was similar in all four groups. Overall, pNR2B gold particles were found in all portions of both presynaptic and postsynaptic compartments in all experimental groups. No abnormalities in overall synapse morphology or

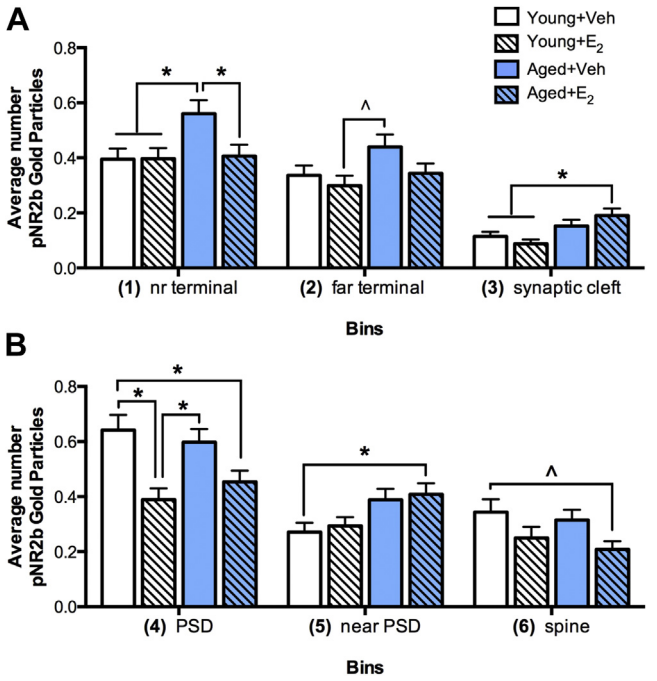

Fig. 5. The distribution of pNR2B gold particles within presynaptic and postsynaptic compartments varied by age and E2 treatment. (A) Presynaptic compartments: On the portion of the terminal near the synapse (bin 1), the number of pNR2B gold particles was significantly greater in aged + Veh females compared to other groups. In the portion of the terminal distal to the synapse (bin 2), the number of pNR2B gold particles tended to be greater in aged + Veh females compared to young + E2 females. In the synaptic cleft (bin 3), the number of pNR2B gold particles in aged + E2 females was significantly greater than both of the young female groups. (B) Postsynaptic compartments: On the PSD of dendritic spines (bin 4), the number of pNR2B gold particles in young and aged + Veh females was significantly more than young + E2 females. Moreover, the number pNR2B gold particles in young + Veh females was significantly more than aged + E2 females on the PSD. In the region of the dendritic spine near the PSD (bin 5), young + Veh females had significantly less pNR2B gold particles than aged + E2 females. In the region of the dendritic spine distal to the PSD regions (bin 6), young + Veh females tended to have more pNR2B gold particles than aged + E2 females. N = 4 rats/group; n ~ 100 synaptic profiles/rat; $^*p < 0.05$; $^\wedge p = 0.05–0.06$. Abbreviations: E2, 17β-estradiol; Veh, vehicle; PSD, postsynaptic density. (For interpretation of the references to color in this figure legend, the reader is referred to the Web version of this article.)

mitochondrial distribution were noted. The total amount of pNR2B gold particles in synaptic complexes was greater in the aged + Veh group compared to all other groups. In the PSD, E2 treatment in the young animals decreased the number of pNR2B gold particles. In the presynaptic terminal, elevated levels of pNR2B particles were found in the aged + Veh group compared to the other three groups. In the postsynaptic compartment, more pNR2B gold particles were observed in the young + Veh and aged + Veh groups compared to their E2 counterparts.

4. Discussion

The aged brain is fundamentally different from the young brain in its capacity for plasticity, particularly in response to estrogen (Adams et al., 2001b; Bean et al., 2014; Milner et al., 2014; Miranda et al., 1999). Moreover, estrogens also affect synaptic communication in brain regions involved in learning and memory, such as the hippocampus, which is of particular importance in the context of human aging when circulating estrogen levels decline and a wide variety of adverse memory-related outcomes are reported (Khoo et al., 2010; Kritz-Silverstein and Barrett-Connor, 2002; McCarrey and Resnick, 2015; Sherwin, 2000). Here, a quantitative analysis of

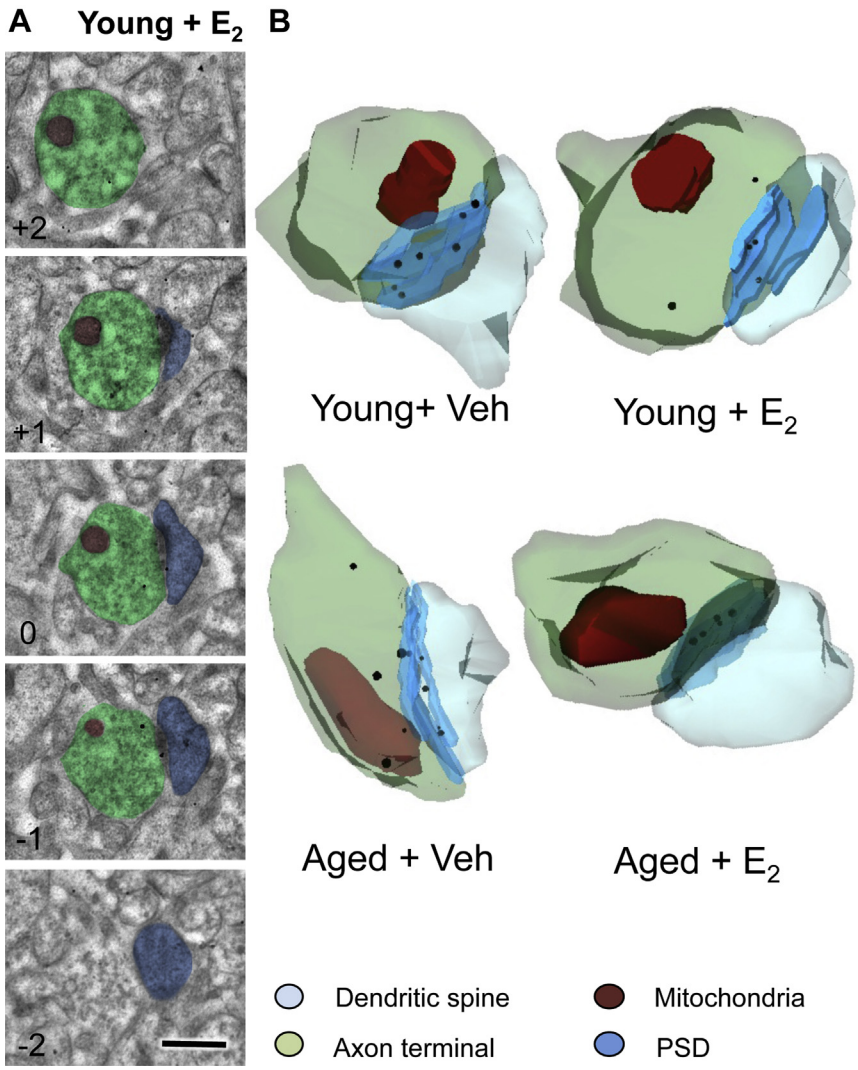

Fig. 6. Three-dimensional reconstruction of representative synaptic complexes from the four groups shows the morphology and subcellular distribution of pNR2B gold particles within the presynaptic and postsynaptic compartment. (A) Representative serial electron micrographs for Young + E2 rats (see Fig. 1 for section numbering scheme). Scale bar = 500 nm. (B) Three-dimensional reconstruction of a representative synaptic complex for each treatment group highlights (1) prominence of mitochondria in the presynaptic terminal; (2) smaller terminal diameter in the young + Veh group compared to young and aged + E2 groups; (3) decreased pNR2B gold particles in the PSD of young animals after E2 exposure; and (4) elevated pNR2B in the presynaptic profile in the aged + Veh groups. Abbreviations: E2, 17β-estradiol; Veh, vehicle; PSD, postsynaptic density. (For interpretation of the references to color in this figure legend, the reader is referred to the Web version of this article.)

the distribution of pNR2B Y1472 in the stratum radiatum of CA1 in young and aged females using postembedding immunocytochemistry and serial section reconstruction suggest that aged synapses as well as mitochondria in synaptic complexes can exhibit youthful-like responses to E2.

4.1. CA1 synapses in young and aged female hippocampus benefited from E2 effects

Overall, E2 replacement had beneficial effects in young and aged females. In axon terminals, the diameter after E2 treatment was increased in both young and aged females compared to young + Veh females. Also, the mitochondria numbers that had decreased by 50% in aged females were restored after E2 to the same levels as young females. In contrast, age rather than E2 had the greater influence on the spine diameter. Age related increase in the spine diameter could reflect the shift in spine morphology from a mixture of all spine types in the young female hippocampus to fewer thin spines in the aged hippocampus [see review: (Hara et al., 2015)]. Differential effects of age and E2 on pNR2B Y1472 depended on its location within the synapse.

Previous examination of NR2A and NR2B demonstrated that young and aged females have similar synaptic levels of both receptor subtypes; however, there is a specific loss of NR2B near the PSD in aged females that is reversed by E2 (Adams et al., 2004). The current examination of pNR2B Y1472 suggests that in the estrogen-deprived state, aged females faired worse than young females as reflected by increased pNR2B levels. However, E2 treatment in aged females reversed elevated pNR2B Y1472 levels throughout the axon terminal and in the PSD to the same levels found in young females. The area of the synapse near the PSD is highly dynamic, but here, pNR2B did not show significant changes with age or E2 treatment.

Duration of estrogen deprivation could have had a bigger effect on synapses in the aged females compared to the young females because the aged females were acyclic before the start of the study. E2 effects on synaptic parameters are affected more by the duration of estrogen deprivation than chronological age (Smith et al., 2010;

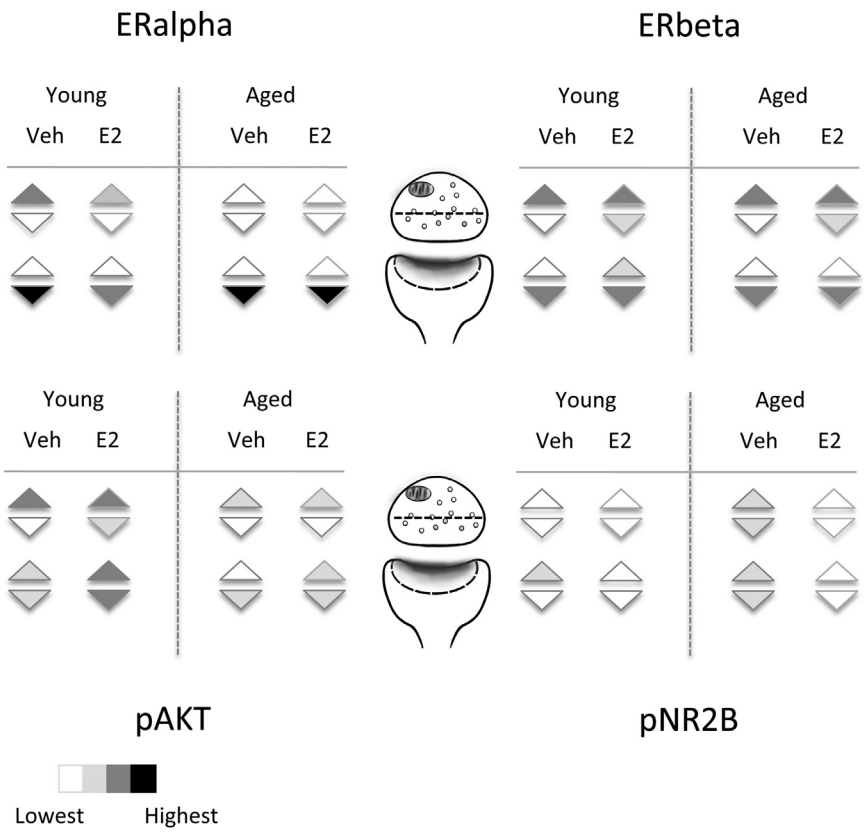

Fig. 7. Schematic diagram summarizing synaptic distribution of pNR2B relative to ERα, ERβ, and pAKT as demonstrated in the same tissue set. In young and aged females, ERβ and pAKT immunoreactivity within CA1 excitatory synapses generally respond to estradiol by changing in the same direction, either increase or decrease, although not always to the same degree so that differences in the overall level do occur. In contrast, in aged females, ERα appears to lose estradiol responsiveness such that the decrease in level seen in young females does not occur. Presynaptically, a decrease in ERα may be undetectable in aged females because the levels are already low. Age results in a new pattern of estrogen regulation for the presynaptic and postsynaptic ion channel NR2B. Phosphorylation of NR2B at Y1427 is impacted by age and sensitive to estradiol replacement. Aged vehicle-treated females had higher levels of pNR2B throughout the synaptic terminal and the dendritic spine compared to young females, which were decreased after estradiol replacement. In young females, pNR2B levels were only affected by estradiol in the postsynaptic compartment closest to the synaptic cleft. Every synapse included in the analysis for all four endpoints contained immunoreactivity for the protein being examined. Expression levels of each are relative only to the protein being represented, direction of change rather than amount is represented. This representation compares proteins closer to the synaptic cleft (<60 nm) to those farther away (>60 nm). Abbreviations: E2, 17β-estradiol; ER, estrogen receptor; Veh, vehicle.

Vedder et al., 2014), and growing evidence suggests that the beneficial effects of E2 replacement decline rapidly as the length of the deprivation grows (Hara et al., 2015; McLaughlin et al., 2008; Smith et al., 2010; Vedder et al., 2014). In addition, as some of the aged rats were retired breeders, this could have influences on the effects of estrogen at the synapses (Barha et al., 2015).

ERs are found in both presynaptic and postsynaptic compartments in the hippocampal neurons and are strongly linked to NMDAR regulation and dependent LTP (Hasegawa et al., 2015; Morissette et al., 2008; Oberlander and Woolley, 2016; Romeo et al., 2005; Smith et al., 2016; Vedder et al., 2013). ER-dependent actions increase both rapid and NMDAR-dependent synaptic transmission in young females along with enhancing memory (Kumar et al., 2015; Smith and McMahon, 2005; Snyder et al., 2011; Vedder et al., 2013; Woolley et al., 1997). Increasing ER expression in aged females restores estrogen effects on memory and NMDAR-dependent LTP (Bean et al., 2015).

Age-related changes in estrogen's ability to maintain synapses, promote synapse formation, and regulate synapse function may be due to changes in ER expression as synaptic ERα decreases but ERβ persists in CA1 synaptic profiles of aged rats (Adams et al., 2002; Waters et al., 2011). Moreover, age-related shifts in estrogen synaptic responses may involve shifts in ERα and ERβ ratios and other components of the rapid signaling cascade, including Ca^{++} dysregulation and alterations in kinase/phosphate activity (Foster, 2012). This, along with ER's ability to connect with direct and indirect modulators of NMDAR potentiation and regulation (Collingridge et al., 2013; Hasegawa et al., 2015; Woolley and McEwen, 1994), suggests that loss of ERs results not only in reductions in estrogen signaling but also alterations in the estrogen signaling pathways that could have far ranging implications for synaptic health during aging.

4.2. Role of NR2B phosphorylation in reported actions of E2

Estrogen's ability to intersect with the cellular mechanisms that regulate NMDAR phosphorylation continues to shed new light on synaptic function and plasticity and animal behavior. Estrogen does not regulate detectable overall levels of NR2B or pNR2B at either the tyrosine (1472 and 1336) or serine (1387, 1303, and 1480) sites (Snyder et al., 2011). However, estrogen enhancement of LTP is NR2B-dependent LTP (Smith et al., 2016; Smith and McMahon, 2006) and others have suggested that estrogens' effects on excitatory synapses likely result from recruitment of NR2B-containing NMDARs to synapses (Snyder et al., 2011). The movement of NR2B-containing NMDARs to synapses is increased by Y1472 phosphorylation of NR2B (Zhang et al., 2008); phosphorylation of Y1472 NR2B is enhanced at the initiation of LTP in

hippocampal CA1 neurons (Nakazawa et al., 2001). However, multiple phosphorylation sites regulate the subcellular localization of NR2B-containing NMDARs through relocation to the surface, stabilization at the surface, and lateral diffusion to extrasynaptic sites (Lussier et al., 2015). Thus, changes in Y1472 pNR2B are likely concurrent with phosphorylation of NR2B at other sites, for example, ser1303 that is regulated by CAMKII phosphorylation (Chen and Roche, 2007), another estrogen-sensitive protein important for induction and maintenance of synaptic plasticity (Logan et al., 2011).

As a result of age or estrogen deprivation, increased or prolonged phosphorylation of Y1472 NR2B could reduce the presynaptic pools of NMDARs. Estrogen deprivation increased presynaptic pNR2B; this effect was reversed by E2 treatment in young females, but not in aged female synapses, suggesting that persistent phosphorylation of NR2B has the potential to alter presynaptic function in aged females due to NMDARs ability to modulate both short- and long-term responses to activity (Duguid and Smart, 2009). Age effects on phosphorylation of NR2B at Y1472 result in reduced receptor diffusion to extrasynaptic sites and blocked internalization (Chen et al., 2012; Gladding et al., 2012; Lussier et al., 2015), ultimately increasing presynaptic pNR2B. Elevated pNR2B may contribute to behavior outcomes as aged mice demonstrate increased phosphorylation of NR2B Y1472 in the prefrontal cortex and no age related deficits in spatial memory (Zamzow et al., 2016). Prolonged surface expression of NMDAR is likely regulated by a number of mechanisms; thus far, Fyn kinase is implicated (Lu et al., 2015), although interactions of estrogen signaling pathways with Fyn kinase remain unexplored. Likewise, aged-related changes in STriatal-Enriched protein tyrosine Phosphatase could contribute to the alterations in synaptic Y1472 phosphorylation of NR2B and memory performance (Cases et al., 2018; Castonguay et al., 2018).

4.3. What this tells us about estrogen, aging, and hippocampal function: potential functional implications

The influences of estrogen on hippocampal-dependent learning and synaptic plasticity are complex, tapping into many cellular processes and exhibiting rapid, short-term, and long-term effects (Kim et al., 2016; Kumar et al., 2015; MacLusky et al., 2005; Sandstrom and Williams, 2004; Tuscher et al., 2016), including NMDAR trafficking (Potier et al., 2016). In the amygdala, phosphorylation of N2B at Tyr-1472 is linked to both chemical and contextual fear learning (Lu et al., 2015). Changes in memory and synapse phenotypes with increased age and estrogen loss (Daniel, 2013; Hara et al., 2015) as well as altered mitochondrial function (Gaignard et al., 2017), together with these findings, further implicate an altered synapse function. With this tissue set, we demonstrated that synaptic protein levels are altered by age and, while aged females may be sensitive to estradiol, the changes may not be consistent with that detected in young, estradiol-treated females (Fig. 7). For pNR2B, aged females did retain most aspects of E2-sensitive responses, although they were not similar to young females across the board. Although cellular and molecular composition of the aged brain diverges from the young brain, the likelihood of beneficial effects of estrogen persists, however, with unique outcomes in aged females and the functional consequences of these differences yet to be explored.

Disclosure statement

The authors declare no competing financial interests.

Acknowledgements

This work was supported by NIH grants AG16765 (JHM, BSM, EMW, and TAM), AG059850 (EMW and TAM), and DA08259 and HL096571 (TAM).

References

Adams, M.M., Morrison, J.H., Gore, A.C., 2001a. N-methyl-D-aspartate receptor mRNA levels change during reproductive senescence in the hippocampus of female rats. Exp. Neurol. 170, 171–179.
Adams, M.M., Oung, T., Morrison, J.H., Gore, A.C., 2001b. Length of postovariectomy interval and age, but not estrogen replacement, regulate N-methyl-D-aspartate receptor mRNA levels in the hippocampus of female rats. Exp. Neurol. 170, 345–356.
Adams, M.M., Shah, R.A., Janssen, W.G., Morrison, J.H., 2001c. Different modes of hippocampal plasticity in response to estrogen in young and aged female rats. Proc. Natl. Acad. Sci. U. S. A 98, 8071–8076.
Adams, M.M., Fink, S.E., Shah, R.A., Janssen, W.G., Hayashi, S., Milner, T.A., McEwen, B.S., Morrison, J.H., 2002. Estrogen and aging affect the subcellular distribution of estrogen receptor-alpha in the hippocampus of female rats. J. Neurosci. 22, 3608–3614.
Adams, M.M., Fink, S.E., Janssen, W.G., Shah, R.A., Morrison, J.H., 2004. Estrogen modulates synaptic N-methyl-D-aspartate receptor subunit distribution in the aged hippocampus. J. Comp. Neurol. 474, 419–426.
Akama, K.T., McEwen, B.S., 2003. Estrogen stimulates postsynaptic density-95 rapid protein synthesis via the AKT/protein kinase B pathway. J. Neurosci. 23, 2333–2339.
Barha, C.K., Lieblich, S.E., Chow, C., Galea, L.A.M., 2015. Multiparity-induced enhancement of hippocampal neurogenesis and spatial memory depends on ovarian hormone status in middle age. Neurobiol. Aging 36, 2391–2405.
Bean, L.A., Ianov, L., Foster, T.C., 2014. Estrogen receptors, the hippocampus, and memory. Neuroscientist 20, 534–545.
Bean, L.A., Kumar, A., Rani, A., Guidi, M., Rosario, A.M., Cruz, P.E., Golde, T.E., Foster, T.C., 2015. Re-opening the critical window for estrogen therapy. J. Neurosci. 35, 16077–16093.
Bourne, J.N., Harris, K.M., 2008. Balancing structure and function at hippocampal dendritic spines. Annu. Rev. Neurosci. 31, 47–67.
Brake, W.G., Alves, S.E., Dunlop, J.C., Lee, S.J., Bulloch, K., Allen, P.B., Greengard, P., McEwen, B.S., 2001. Novel target sites for estrogen action in the dorsal hippocampus: an examination of synaptic proteins. Endocrinology 142, 1284–1289.
Cases, S., Saavedra, A., Tyebji, S., Giralt, A., Alberch, J., Perez-Navarro, E., 2018. Age-related changes in striatal-enriched protein tyrosine phosphatase levels: regulation by BDNF. Mol. Cell Neurosci 86, 41–49.
Castonguay, D., Dufort-Gervais, J., Menard, C., Chatterjee, M., Quirion, R., Bontempi, B., Schneider, J.S., Arnsten, A.F.T., Nairn, A.C., Norris, C.M., Ferland, G., Bezard, E., Gaudreau, P., Lombroso, P.J., Brouillette, J., 2018. The tyrosine phosphatase step is involved in age-related memory decline. Curr. Biol. 28, 1079–1089 e1074.
Chen, B.S., Roche, K.W., 2007. Regulation of NMDA receptors by phosphorylation. Neuropharmacology 53, 362–368.
Chen, B.S., Gray, J.A., Sanz-Clemente, A., Wei, Z., Thomas, E.V., Nicoll, R.A., Roche, K.W., 2012. Sap102 mediates synaptic clearance of NMDA receptors. Cell Rep 2, 1120–1128.
Chen, Y., Chen, A.Q., Luo, X.Q., Guo, L.X., Tang, Y., Bao, C.J., Lin, L., Lin, C., 2014. Hippocampal NR2B-containing NMDA receptors enhance long-term potentiation in rats with chronic visceral pain. Brain Res. 1570, 43–53.
Collingridge, G.L., Volianskis, A., Bannister, N., France, G., Hanna, L., Mercier, M., Tidball, P., Fang, G., Irvine, M.W., Costa, B.M., Monaghan, D.T., Bortolotto, Z.A., Molnar, E., Lodge, D., Jane, D.E., 2013. The NMDA receptor as a target for cognitive enhancement. Neuropharmacology 64, 13–26.
Crimins, J.L., Wang, A.C., Yuk, F., Puri, R., Janssen, W.G.M., Hara, Y., Rapp, P.R., Morrison, J.H., 2017. Diverse synaptic distributions of G protein-coupled estrogen receptor 1 in monkey prefrontal cortex with aging and menopause. Cereb. Cortex 27, 2022–2033.
Cull-Candy, S.G., Leszkiewicz, D.N., 2004. Role of distinct NMDA receptor subtypes at central synapses. Sci. STKE 2004, re16.
Daniel, J.M., 2013. Estrogens, estrogen receptors, and female cognitive aging: the impact of timing. Horm. Behav. 63, 231–237.
Duguid, I.C., Smart, T.G., 2009. Presynaptic NMDA Receptors Biology of the NMDA Receptor. Taylor & Francis Group, LLC, Boca Raton FL.
Foster, T.C., 2012. Role of estrogen receptor alpha and beta expression and signaling on cognitive function during aging. Hippocampus 22, 656–669.
Foster, T.C., Kyritsopoulos, C., Kumar, A., 2017. Central role for NMDA receptors in redox mediated impairment of synaptic function during aging and alzheimer's disease. Behav. Brain Res. 322, 223–232.
Funabashi, T., Kleopoulos, S.P., Kimura, F., Mobbs, C.V., 1998. Changes in neurotensin mRNA by estrogen in the female rat preoptic area during aging: an in situ hybridization histochemistry study. Gen. Comp. Endocrinol. 112, 364–371.
Gaignard, P., Liere, P., Therond, P., Schumacher, M., Slama, A., Guennoun, R., 2017. Role of sex hormones on brain mitochondrial function, with special reference to aging and neurodegenerative diseases. Front Aging Neurosci. 9, 406.

Gladding, C.M., Sepers, M.D., Xu, J., Zhang, L.Y., Milnerwood, A.J., Lombroso, P.J., Raymond, L.A., 2012. Calpain and striatal-enriched protein tyrosine phosphatase (step) activation contribute to extrasynaptic NMDA receptor localization in a Huntington's disease mouse model. Hum. Mol. Genet. 21, 3739–3752.
Guidi, M., Rani, A., Karic, S., Severance, B., Kumar, A., Foster, T.C., 2015. Contribution of N-methyl-D-aspartate receptors to attention and episodic spatial memory during senescence. Neurobiol. Learn Mem. 125, 36–46.
Hao, J., Janssen, W.G., Tang, Y., Roberts, J.A., McKay, H., Lasley, B., Allen, P.B., Greengard, P., Rapp, P.R., Kordower, J.H., Hof, P.R., Morrison, J.H., 2003. Estrogen increases the number of spinophilin-immunoreactive spines in the hippocampus of young and aged female rhesus monkeys. J. Comp. Neurol. 465, 540–550.
Hara, Y., Yuk, F., Puri, R., Janssen, W.G., Rapp, P.R., Morrison, J.H., 2014. Presynaptic mitochondrial morphology in monkey prefrontal cortex correlates with working memory and is improved with estrogen treatment. Proc. Natl. Acad. Sci. U. S. A 111, 486–491.
Hara, Y., Waters, E.M., McEwen, B.S., Morrison, J.H., 2015. Estrogen effects on cognitive and synaptic health over the lifecourse. Physiol. Rev. 95, 785–807.
Hasegawa, Y., Hojo, Y., Kojima, H., Ikeda, M., Hotta, K., Sato, R., Ooishi, Y., Yoshiya, M., Chung, B.C., Yamazaki, T., Kawato, S., 2015. Estradiol rapidly modulates synaptic plasticity of hippocampal neurons: involvement of kinase networks. Brain Res. 1621, 147–161.
Hicklin, T.R., Wu, P.H., Radcliffe, R.A., Freund, R.K., Goebel-Goody, S.M., Correa, P.R., Proctor, W.R., Lombroso, P.J., Browning, M.D., 2011. Alcohol inhibition of the NMDA receptor function, long-term potentiation, and fear learning requires striatal-enriched protein tyrosine phosphatase. Proc. Natl. Acad. Sci. U. S. A 108, 6650–6655.
Hunt, D.L., Castillo, P.E., 2012. Synaptic plasticity of NMDA receptors: mechanisms and functional implications. Curr. Opin. Neurobiol. 22, 496–508.
Janssen, W.G., Vissavajjhala, P., Andrews, G., Moran, T., Hof, P.R., Morrison, J.H., 2005. Cellular and synaptic distribution of NR2A and NR2B in macaque monkey and rat hippocampus as visualized with subunit-specific monoclonal antibodies. Exp. Neurol. 191 (Suppl 1), S28–S44.
Khoo, S.K., O'Neill, S., Byrne, G., King, R., Travers, C., Tripcony, L., 2010. Postmenopausal hormone therapy and cognition: effects of timing and treatment type. Climacteric 13, 259–264.
Kim, J., Szinte, J.S., Boulware, M.I., Frick, K.M., 2016. 17beta-estradiol and agonism of G-protein-coupled estrogen receptor enhance hippocampal memory via different cell-signaling mechanisms. J. Neurosci. 36, 3309–3321.
Kramar, E.A., Babayan, A.H., Gall, C.M., Lynch, G., 2013. Estrogen promotes learning-related plasticity by modifying the synaptic cytoskeleton. Neuroscience 239, 3–16.
Kritz-Silverstein, D., Barrett-Connor, E., 2002. Hysterectomy, oophorectomy, and cognitive function in older women. J. Am. Geriatr. Soc. 50, 55–61.
Kumar, A., Bean, L.A., Rani, A., Jackson, T., Foster, T.C., 2015. Contribution of estrogen receptor subtypes, ERalpha, ERbeta, and GPER1 in rapid estradiol-mediated enhancement of hippocampal synaptic transmission in mice. Hippocampus 25, 1556–1566.
Lauber, A.H., Romano, G.J., Mobbs, C.V., Howells, R.D., Pfaff, D.W., 1990. Estradiol induction of proenkephalin messenger RNA in hypothalamus: Dose-response and relation to reproductive behavior in the female rat. Brain Res. Mol. Brain Res. 8, 47–54.
Lee, K.F., Soares, C., Beique, J.C., 2012. Examining form and function of dendritic spines. Neural Plast. 2012, 704103.
Lewis, M.C., Kerr, K.M., Orr, P.T., Frick, K.M., 2008. Estradiol-induced enhancement of object memory consolidation involves NMDA receptors and protein kinase A in the dorsal hippocampus of female C57BL/6 mice. Behav. Neurosci. 122, 716–721.
Logan, S.M., Sarkar, S.N., Zhang, Z., Simpkins, J.W., 2011. Estrogen-induced signaling attenuates soluble Aβ peptide-mediated dysfunction of pathways in synaptic plasticity. Brain Res. 1383, 1–12.
Lu, W., Fang, W., Li, J., Zhang, B., Yang, Q., Yan, X., Peng, L., Ai, H., Wang, J.J., Liu, X., Luo, J., Yang, W., 2015. Phosphorylation of tyrosine 1070 at the GluN2B subunit is regulated by synaptic activity and critical for surface expression of N-methyl-D-aspartate (NMDA) receptors. J. Biol. Chem. 290, 22945–22954.
Lussier, M.P., Sanz-Clemente, A., Roche, K.W., 2015. Dynamic regulation of N-methyl-D-aspartate (NMDA) and alpha-amino-3-hydroxy-5-methyl-4-isoxazolepropionic acid (AMPA) receptors by posttranslational modifications. J. Biol. Chem. 290, 28596–28603.
MacDonald, J.F., Jackson, M.F., Beazely, M.A., 2006. Hippocampal long-term synaptic plasticity and signal amplification of NMDA receptors. Crit. Rev. Neurobiol. 18, 71–84.
MacLusky, N.J., Luine, V.N., Hajszan, T., Leranth, C., 2005. The 17alpha and 17beta isomers of estradiol both induce rapid spine synapse formation in the ca1 hippocampal subfield of ovariectomized female rats. Endocrinology 146, 287–293.
McCarrey, A.C., Resnick, S.M., 2015. Postmenopausal hormone therapy and cognition. Horm. Behav. 74, 167–172.
McLaughlin, K.J., Bimonte-Nelson, H., Neisewander, J.L., Conrad, C.D., 2008. Assessment of estradiol influence on spatial tasks and hippocampal CA1 spines: evidence that the duration of hormone deprivation after ovariectomy compromises 17beta-estradiol effectiveness in altering CA1 spines. Horm. Behav. 54, 386–395.
Milner, T.A., McEwen, B.S., Waters, E.M., 2014. Estrogen effects on hippocampal synapses. Chapter 7 pp. 195-219. In: Pickel, V.M., Segal, M. (Eds.), Structure and function of the synapse, Book 3 in the Neuroscience Net Reference Book Series. Neuroscience-Net, Redwood City, CA. J. Johnson Managing Editor. http://www.neuroscience.com.
Miranda, P., Williams, C.L., Einstein, G., 1999. Granule cells in aging rats are sexually dimorphic in their response to estradiol. J. Neurosci. 19, 3316–3325.
Moon, I.S., Apperson, M.L., Kennedy, M.B., 1994. The major tyrosine-phosphorylated protein in the postsynaptic density fraction is N-methyl-D-aspartate receptor subunit 2B. Proc. Natl. Acad. Sci. U. S. A 91, 3954–3958.
Morissette, M., Le Saux, M., Di Paolo, T., 2008. Effect of oestrogen receptor alpha and beta agonists on brain N-methyl-D-aspartate receptors. J. Neuroendocrinol 20, 1006–1014.
Nakazawa, T., Komai, S., Tezuka, T., Hisatsune, C., Umemori, H., Semba, K., Mishina, M., Manabe, T., Yamamoto, T., 2001. Characterization of fyn-mediated tyrosine phosphorylation sites on glur epsilon 2 (NR2B) subunit of the N-methyl-D-aspartate receptor. J. Biol. Chem. 276, 693–699.
Nong, Y., Huang, Y.Q., Salter, M.W., 2004. NMDA receptors are movin' in. Curr. Opin. Neurobiol. 14, 353–361.
Oberlander, J.G., Woolley, C.S., 2016. 17beta-estradiol acutely potentiates glutamatergic synaptic transmission in the hippocampus through distinct mechanisms in males and females. J. Neurosci. 36, 2677–2690.
Potier, M., Georges, F., Brayda-Bruno, L., Ladepeche, L., Lamothe, V., Al Abed, A.S., Groc, L., Marighetto, A., 2016. Temporal memory and its enhancement by estradiol requires surface dynamics of hippocampal CA1 N-methyl-D-aspartate receptors. Biol. Psychiatry 79, 735–745.
Prybylowski, K., Chang, K., Sans, N., Kan, L., Vicini, S., Wenthold, R.J., 2005. The synaptic localization of NR2B-containing NMDA receptors is controlled by interactions with PDZ proteins and AP-2. Neuron 47, 845–857.
Romeo, R.D., McCarthy, J.B., Wang, A., Milner, T.A., McEwen, B.S., 2005. Sex differences in hippocampal estradiol-induced N-methyl-D-aspartic acid binding and ultrastructural localization of estrogen receptor-alpha. Neuroendocrinology 81, 391–399.
Sandstrom, N.J., Williams, C.L., 2004. Spatial memory retention is enhanced by acute and continuous estradiol replacement. Horm. Behav. 45, 128–135.
Sherwin, B.B., 2000. Oestrogen and cognitive function throughout the female lifespan. Novartis Found Symp. 230, 188–196 discussion 196-201.
Smith, C.C., McMahon, L.L., 2005. Estrogen-induced increase in the magnitude of long-term potentiation occurs only when the ratio of NMDA transmission to AMPA transmission is increased. J. Neurosci. 25, 7780–7791.
Smith, C.C., McMahon, L.L., 2006. Estradiol-induced increase in the magnitude of long-term potentiation is prevented by blocking NR2B-containing receptors. J. Neurosci. 26, 8517–8522.
Smith, C.C., Vedder, L.C., Nelson, A.R., Bredemann, T.M., McMahon, L.L., 2010. Duration of estrogen deprivation, not chronological age, prevents estrogen's ability to enhance hippocampal synaptic physiology. Proc. Natl. Acad. Sci. U. S. A 107, 19543–19548.
Smith, C.C., Smith, L.A., Bredemann, T.M., McMahon, L.L., 2016. 17beta estradiol recruits GluN2B-containing NMDARs and ERK during induction of long-term potentiation at temporoammonic-CA1 synapses. Hippocampus 26, 110–117.
Snyder, M.A., Cooke, B.M., Woolley, C.S., 2011. Estradiol potentiation of NR2B-dependent EPSCs is not due to changes in NR2B protein expression or phosphorylation. Hippocampus 21, 398–408.
Takasu, M.A., Dalva, M.B., Zigmond, R.E., Greenberg, M.E., 2002. Modulation of NMDA receptor- dependent calcium influx and gene expression through EPHB receptors. Science 295, 491–495.
Tuscher, J.J., Luine, V., Frankfurt, M., Frick, K.M., 2016. Estradiol-mediated spine changes in the dorsal hippocampus and medial prefrontal cortex of ovariectomized female mice depend on ERK and mTOR activation in the dorsal hippocampus. J. Neurosci. 36, 1483–1489.
Van Lookeren Campagne, M., Oestreicher, A.B., Buma, P., Verkleij, A.J., Gispen, W.H., 1991. Ultrastructural localization of adrenocorticotrophic hormone and the phosphoprotein B-50/growth-associated protein 43 in freeze-substituted, lowicryl HM20-embedded mesencephalic central gray substance of the rat. Neuroscience 42, 517–529.
Vedder, L.C., Smith, C.C., Flannigan, A.E., McMahon, L.L., 2013. Estradiol-induced increase in novel object recognition requires hippocampal NR2B-containing NMDA receptors. Hippocampus 23, 108–115.
Vedder, L.C., Bredemann, T.M., McMahon, L.L., 2014. Estradiol replacement extends the window of opportunity for hippocampal function. Neurobiol. Aging 35, 2183–2192.
Waters, E.M., Mitterling, K., Spencer, J.L., Mazid, S., McEwen, B.S., Milner, T.A., 2009. Estrogen receptor alpha and beta specific agonists regulate expression of synaptic proteins in rat hippocampus. Brain Res. 1290, 1–11.
Waters, E.M., Yildirim, M., Janssen, W.G., Lou, W.Y., McEwen, B.S., Morrison, J.H., Milner, T.A., 2011. Estrogen and aging affect the synaptic distribution of estrogen receptor beta-immunoreactivity in the CA1 region of female rat hippocampus. Brain Res. 1379, 86–97.
Woolley, C.S., McEwen, B.S., 1992. Estradiol mediates fluctuation in hippocampal synapse density during the estrous cycle in the adult rat. J. Neurosci. 12, 2549–2554.
Woolley, C.S., McEwen, B.S., 1994. Estradiol regulates hippocampal dendritic spine density via an N-methyl-D-aspartate receptor-dependent mechanism. J. Neurosci. 14, 7680–7687.
Woolley, C.S., Weiland, N.G., McEwen, B.S., Schwartzkroin, P.A., 1997. Estradiol increases the sensitivity of hippocampal CA1 pyramidal cells to NMDA receptor-mediated synaptic input: correlation with dendritic spine density. J. Neurosci. 17, 1848–1859.

Yildirim, M., Janssen, W.G., Tabori, N.E., Adams, M.M., Yuen, G.S., Akama, K.T., McEwen, B.S., Milner, T.A., Morrison, J.H., 2008. Estrogen and aging affect synaptic distribution of phosphorylated LIM kinase (pLIMk) in CA1 region of female rat hippocampus. Neuroscience 152, 360–370.

Youle, R.J., van der Bliek, A.M., 2012. Mitochondrial fission, fusion, and stress. Science 337, 1062–1065.

Zamzow, D.R., Elias, V., Acosta, V.A., Escobedo, E., Magnusson, K.R., 2016. Higher levels of phosphorylated y1472 on GluN2B subunits in the frontal cortex of aged mice are associated with good spatial reference memory, but not cognitive flexibility. Age (Dordr) 38, 50.

Zhang, S., Edelmann, L., Liu, J., Crandall, J.E., Morabito, M.A., 2008. Cdk5 regulates the phosphorylation of tyrosine 1472 NR2B and the surface expression of NMDA receptors. J. Neurosci. 28, 415–424.

Znamensky, V., Akama, K.T., McEwen, B.S., Milner, T.A., 2003. Estrogen levels regulate the subcellular distribution of phosphorylated AKT in hippocampal CA1 dendrites. J. Neurosci. 23, 2340–2347.